Panorama Based Point Cloud Reduction

Hamidreza Houshiar, Dorit Borrmann, Jan Elseberg and Andreas Nüchter

***Abstract*— To reconstruct environments 3D point clouds acquired by laser scanners are registered. This is an important but also time consuming part of any mapping system for mobile robots. The time needed for mapping is drastically reduced when the size of the input data is reduced. This paper examines different ways of reducing the size of point clouds without losing vital information for the matching process. We present novel point cloud reduction methods on the basis of panorama images. It is shown that the reduced point clouds are ideally suited for feature based registration on panorama images. We evaluate the presented reduction methods based on their effect on the performance of the registration algorithm.**

I. INTRODUCTION

Laser scanners are used in modeling 3D structures, for object detection, digitizing entire cities and landscapes. A 3D laser scanner creates an image of its surrounding by scanning it with laser beams thus acquiring a 3D point cloud. Digitizing environments without occlusions requires multiple 3D scans. Scan registration is the process of creating a correct and consistent model by merging the coordinate systems of several scans.

2D laser scanners use a rotating mirror to deflect the emitted laser beam and measure the distance r to an object under a certain angle φ. The polar representation (φ, r) of a surface profile can be transformed into Cartesian coordinates.

The authors are with the Automation group at the School of Engineering and Science, Jacobs University Bremen gGmbH, 28759 Bremen, Germany (h.houshiar|d.borrmann|j.elseberg|a.nuechter)@jacobs-university.de

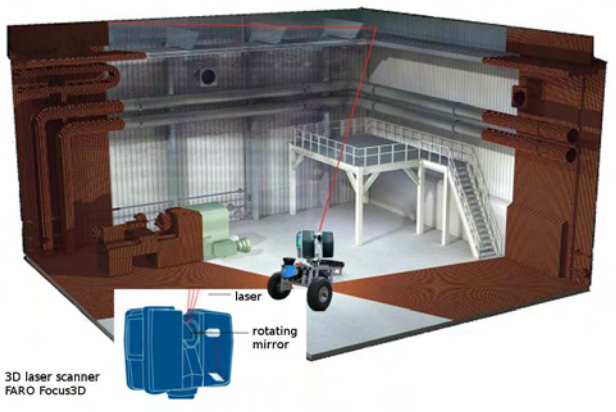

Fig. 1: Illustration of a 3D scan with a FARO Focus3D laser scanner. The scanner gages up to 976000 points/sec on a sphere around it by a rotating mirror and a second rotation around the vertical axis. The background image is courtesy of FARO.

)

3D laser scanners either use a second mirror or rotate a 2D laser scanner to generate 3D point clouds of the scanned environment (cf. Fig. 1). The resulting 3D data in spherical coordinates (θ, φ, r), with θ as the angle of the second rotation, can again be transformed into Cartesian coordinates (x, y, z).

Data acquisition with 3D laser scanner is virtually unlimited with respect to resolution. Modern laser scanners can acquire more than a million points per second. This leads to point clouds with large numbers of points. Data reduction becomes necessary to efficiently perform operations on these point clouds. Reduced point clouds will notably increase the speed of the registration process. In this paper we will discuss scan reduction for this task.

Most of recent terrestrial laser scanners provide reflectance and sometimes even color data in addition to range information. This data can be used to generate panorama images from the acquired 3D scans. Image generation from point clouds will allow for applying the conventional 2D image matching algorithms to point clouds.

Böhm et al. explore the application of the scale invariant feature transform (SIFT) method on laser reflectance data [1]. In our previous work we study the different projections for key point based registration of panoramic terrestrial 3D laser scans [2]. In the following we will present several panorama generation methods and exploit their ability to reduce point clouds to speed up the registration process. The methods are contrasted with a state of the art reduction method based on octrees.

II. STATE OF THE ART

Generating 3D models of structures, objects and environments requires multiple 3D scans. Rigid 3D models are created from the registration of several scans. This process requires selection of initial feature or point correspondences for every two acquired scan pairs. The relative orientation between scan pairs is computed with the aforementioned correspondences.

In automatic pairwise scan-to-scan registration methods the transformation matrix between two corresponding scan pairs is computed based on automatically detected similarities in the point clouds. These similarities rely either purely on points or on features in the scans.

Point based registration methods register 3D point clouds by selecting point correspondences. These algorithms require no computation of features. The Iterative Closest Point (ICP) algorithm is a well known algorithm for point based registration [3]. It works for point correspondences on the basis of smallest distance and minimizing the resulting Euclidean

error. The algorithm converges to a local minimum. Good start estimate are essential for good matching results. These start estimates can be produced by feature based algorithms. The fine registration is then achieved by the ICP algorithm.

There are methods based on natural features that are generated automatically from 3D point clouds. These features are exploited to find correspondences between scan pairs. Hansen et al. consider an application of scale-invariant feature detection using scale-space analysis [4], [5]. Böhm and Becker suggest the use of scale invariant feature transform (SIFT) features for automatic registration [1]. Wang and Brenner extend this work by using additional geometry features to reduce the number of matching outliers in panoramic outdoor scans [6]. Weinmann et al. present a method that is based on both range and reflectance information of 3D point clouds [7], [8]. These approaches extract the correspondences for registration based on features extracted both from the images and directly from the 3D point cloud. In our previous work we proposed an approach to convert 3D scans into panorama images, extract features from the images. We used conventional 2D feature detectors and descriptors to extract the correspondences for scan pairs, such as the scale invariant feature transform (SIFT) [9], speed-up robust features (SURF) [10] and others ([11], [12], [13], [14]). The transformation matrix is computed by using RANSAC and a least squares method [2].

There are approaches for reducing the complexity of scan registration by extracting planes from the data [15], [16]. However, by using geometrical features the precise point measurements are lost. Little work has been done on subsampling 3D point clouds, e.g., by using range images [17]. Other methods for reducing the size of point clouds separate the space into voxels and sample points from each voxel. Efficient methods with uniform voxels use octrees [18]. Similarly Lee subdivides the point cloud into a non-uniform grid based on normals [19]. Suter et al. cluster the data with a k-nearest neighbor approach to remove points from the original data [20]. Methods that use multiple scans to reduce redundancies such as the method proposed by Swadzba et. al. [21] cannot be used for registration as they require knowledge about correspondences beforehand.

III. PANORAMA GENERATION

Range and reflectance information from the acquired scans are used for the generation of the panoramic images. On these images we utilize 2D feature detector and description methods for 3D scan registration. The scanned environment can be considered as projected to a sphere with the scanner positioned in the center of the sphere. Panorama generation is the process of mapping the spherical coordinates θ, φ, r of the points to the image coordinates x and y.

A. EQUIRECTANGULAR

The equirectangular projection is the simplest projection and is used in many applications to map a portion of a surface of a sphere to a flat image. With this projection the longitude and latitude are mapped to horizontal and vertical coordinates of a grid with no transformation or scaling applied. In an equirectangular projected image all vertical straight lines remain vertical and straight, however horizontal straight lines will become curves expect the horizon. This projection supports 360° in the horizontal field of view and 180° in the vertical field of view. Coordinates relate linearly to θ and φ. Poles in this projection are stretched to the entire width of the image at the top and bottom edges. The transformation equations of this projection are:

$$x = \theta \tag{1a}$$

$$y = \varphi, \tag{1b}$$

where the longitude θ and the latitude φ are the spherical coordinates (see Figure 2).

B. CYLINDRICAL

The cylindrical projection can be envisioned by wrapping a flat piece of paper around the circumference of a sphere, such that it is a sphere tangent to the equator of the sphere. Emitting light from the center of the sphere will project the sphere onto the cylinder.This projection is similar to the equirectangular projection. Straight vertical lines remain straight, and horizontal lines become curves. Objects are stretched vertically, especially those close to the north and south pole of the sphere. The vertical field of view is restricted to 120° or less. However, it has the same recommended horizontal field of view as the equirectangular projection which is a field of view between 120° and 360° (see Figure 2). The noticeable distortion of this projection is mostly on the top and the bottom of the mapped image. For outdoor scenarios this is mostly the sky and the ground. Therefore distortions have little effect on the feature detection process in outdoor scenarios. To map the panorama data onto the image, the projection proceeds as:

$$x = \theta \tag{2a}$$

$$y = \tan\varphi. \tag{2b}$$

C. MERCATOR

The Mercator projection is related to the equirectangular projection and the cylindrical projection. It shows less pronounced distortions compared to the aforementioned projections. The Mercator projection is a conformal projection. It has less vertical stretching and a greater field of view. A variation of this projection is often used for very tall vertical panoramas. The Mercator projection is recommended for a horizontal field of view between 120° and 360° and a vertical field of view less than 150°. This projection is an isogonic projection, i.e., angles are preserved. It proceeds as:

$$x = \theta \tag{3a}$$

$$y = \ln\left(\tan\varphi + \frac{1}{\cos\varphi}\right), \tag{3b}$$

mapping the longitude θ to horizontal coordinates and calculating the vertical coordinates of the image (see Figure 2).

D. RECTILINEAR

The rectilinear projection can be imagined by placing a piece of flat paper tangent to a sphere at a single point and illuminating the surface from the center of the sphere. The projected image to the paper is the rectilinear projection of the portion of the sphere onto the flat image.This projection maps the straight lines in 3D space to straight lines in the 2D image. It has a smaller field of view as compared to the aforementioned projections. The image is stretched towards the corners and the distortion grows with larger fields of view (see Figure 2). The projection proceeds as:

$$x = \frac{\cos\varphi \sin(\theta - \theta_0)}{\sin\varphi_1 \sin\varphi + \cos\varphi_1 \cos\varphi \cos(\theta - \theta_0)} \tag{4a}$$

$$y = \frac{\cos\varphi_1 \sin\varphi - \sin\varphi_1 \cos\varphi \cos(\theta - \theta_0)}{\sin\varphi_1 \sin\varphi + \cos\varphi_1 \cos\varphi \cos(\theta - \theta_0)}. \tag{4b}$$

The recommended horizontal and vertical field of view for this projection is less than $120°$. The generation of a $360°$ panorama image requires multiple rectilinear projected images. One can generate three rectilinear projected images with $120°$ field of view and merge them respectively to produce a full $360°$ panorama image.

E. PANNINI

The Pannini projection is a mathematical rule for constructing perspective images with a very large field of view. It can be imagined as a rectilinear projection of a 3D cylindrical image. This image is itself a projection of the sphere onto a tangent cylinder. The center of the rectilinear projection can vary and is on the viewing axis at distance d from the cylinder axis. For $d = 0$ the projection is rectilinear and for $d \to \infty$ it gives the cylindrical orthographic projection. The projection with $d = 1$ has been defined as the Pannini projection. The images produced by the Pannini projection have a single central vanishing point. The images appear to have a correct perspective even when using a wide field of view. These images often resemble a normal rectilinear perspective. The horizontal field of view can be larger than for rectilinear projection, without the noticeable distortions at the edges in the rectilinear projection. Straight vertical lines remain straight and the radial lines through the center of the image stay straight. However, it transforms horizontal lines into curves (see Figure 2). The recommended vertical and horizontal field of view for the Pannini projection is less than $150°$. Therefore, the projection demands dividing a $360°$ scan into several sub-sets. The projection proceeds as:

$$x = \frac{(d+1)\sin(\theta - \theta_0)}{d + \sin\varphi_1 \tan\varphi + \cos\varphi_1 \cos(\theta - \theta_0)} \tag{5a}$$

$$y = \frac{(d+1)\tan\varphi \left(\cos\varphi_1 - \sin\varphi_1 \left(\frac{1}{\tan\varphi}\right) \cos(\theta - \theta_0)\right)}{d + \sin\varphi_1 \tan\varphi + \cos\varphi_1 \cos(\theta - \theta_0)}. \tag{5b}$$

For the original Pannini projection the projection center was assumed to be at the south pole ([22]). The equations given here are modified to allow for different projection centers. Thus θ_0 and φ_1 are the projection center in each subset of the data.

F. STEROGRAPHIC

The sterographic projection can be imagined by placing a flat paper tangent to a sphere and illuminating it from the other pole. Each point on the sphere casts a shadow on the paper. One pole is the center of the projection. Latitude lines appear as circles around the central point. Distortions increase further from the pole up to the equator. The equator is increased twice in size compared to the sphere. The other hemisphere of the sphere is stretched even more through the pole where it is mapped to infinity. However, the center of the projection and the illuminating point are not bound to the poles of the sphere. The center of the point can be any point on the sphere. The illuminating point can have any distance R from the central point. Images over $330°$ are not very functional. The recommended horizontal and vertical field of view for this projection is less than $120°$. In order to satisfy the essentials of this projection dividing a $360°$ scan to sub-sets is required, and the projection proceeds as:

$$x = \frac{2R\cos\varphi \sin(\theta - \theta_0)}{1 + \sin\varphi_1 \sin\varphi + \cos\varphi_1 \cos\varphi \cos(\theta - \theta_0)} \tag{6a}$$

$$y = \frac{2R\left(\cos\varphi_1 \sin\varphi - \sin\varphi_1 \cos\varphi \cos(\theta - \theta_0)\right)}{1 + \sin\varphi_1 \sin\varphi + \cos\varphi_1 \cos\varphi \cos(\theta - \theta_0)}, \tag{6b}$$

where θ_0 and φ_1 are the projection centers in each data subset (see Figure 2). The R parameter is any non negative value. $R = 1$ generates the Pannini projection. High values for R introduce more distortion. We use $R = 2$ in our experiments.

G. ALBERS EQUAL-AREA CONIC

The Albers equal-area conic projection can be imagined as a map wrapped onto a cone set over the sphere. The cone intersects the sphere at one or two latitude lines called standard lines. The term conic is referred to any projection in which longitudes are mapped to equally distanced lines, converging at a point which may or not be a pole. Circles of latitude are mapped to arcs of circles, concentric in the point of convergence of longitude lines. The resulting map has low distortion in scale, shape and area near these standard lines. Equal area projections are projections that preserve the area. The Albers equal-area conic projection has little distortions along the central latitude and none at the standard lines. This projection is suited for those areas on the sphere that extend from east to west rather than those from north to south. In this projection the $90°$ angles between latitudes and longitudes are preserved. However, since the scale along the lines of longitude does not match the scale along the lines of latitude, the projection is not conformal. This projection is recommended for a horizontal field of view up to $360°$ and a

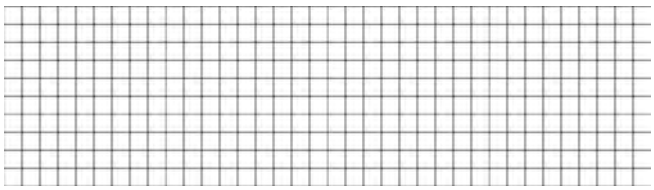

(a) Latitude and longitude map with equirectangular projection

(b) Reflectance map with equirectangular projection

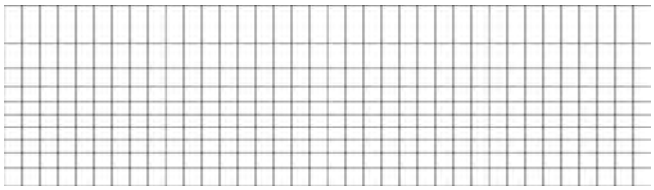

(c) Latitude and longitude map with cylindrical projection

(d) Reflectance map with cylindrical projection

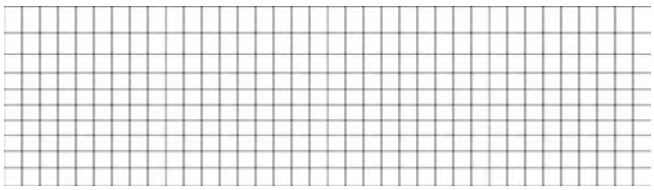

(e) Latitude and longitude map with Mercator projection

(f) Reflectance map with Mercator projection

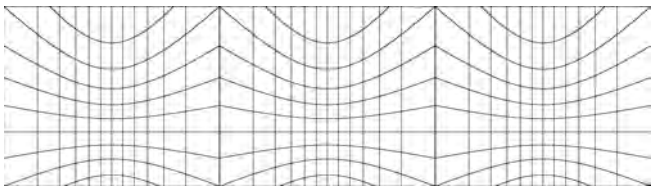

(g) Latitude and longitude map with rectilinear projection

(h) Reflectance map with rectilinear projection

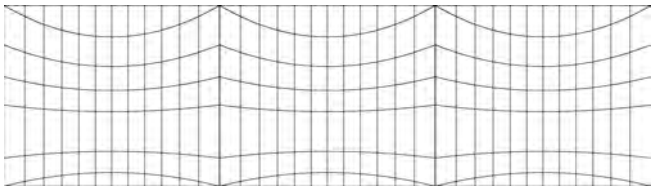

(i) Latitude and longitude map with Pannini projection

(j) Reflectance map with Pannini projection

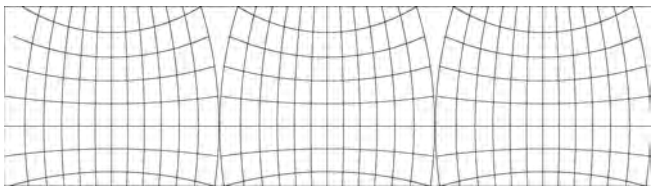

(k) Latitude and longitude map with stereographic projection

(l) Reflectance map with stereographic projection

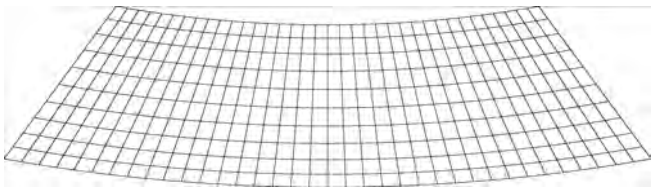

(m) Latitude and longitude map with Albers equal-area conic projection

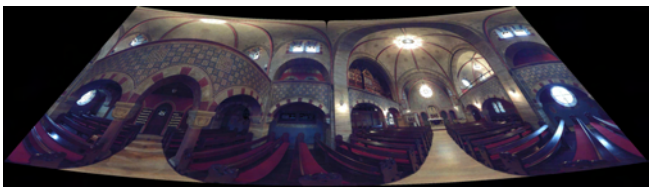

(n) Reflectance map with Albers equal-area conic projection

Fig. 2: Panorama projections

vertical field of view less than $60°$. The projection proceeds as:

$$x = \rho \sin\theta \tag{7a}$$

$$y = \rho_0 - \rho \cos\theta, \tag{7b}$$

where

$$n = \frac{1}{2}(\sin\varphi_1 + \sin\varphi_2) \tag{8a}$$

$$\theta = n(\lambda - \lambda_0) \tag{8b}$$

$$C = \cos^(2)\varphi_1 + 2n\sin\varphi_1 \tag{8c}$$

$$\rho = \frac{\sqrt{C - 2n\sin\varphi}}{n} \tag{8d}$$

$$\rho_0 = \frac{\sqrt{C - 2n\sin\varphi_0}}{n}. \tag{8e}$$

The φ_0 and λ_0 are the latitude and longitude of the origin of the cartesian coordinates. The φ_1 and φ_2 are the standard lines (see Figure 2). In our experiments we have utilized $(\varphi_0, \lambda_0) = (0°, 0°)$ and the standard lines at $\varphi_1 = -40°$ and $\varphi_2 = 60°$.

IV. AUTOMATIC REGISTRATION

For the automatic registration of point clouds using these panoramas, features are extracted for each scan. These correspondences are used to generate pairwise transformation matrices with a RANSAC-like [23] approach. The registration matches features from the two panorama images of a scan pair, i.e., identifies features in one image that is closest to the sampled feature from the other image based on a comparison of their descriptors. Several algorithms such as $k-$nearest neighbor (KNN) search and radius KNN search are possible solutions to this problem. The ratio nearest search as presented by [9] has shown the most promising results. The registration proceeds by testing a subset of 3 point pair matches and examining the two triangles that are defined by these points. The algorithm translates the triangles so that their centroids lie at the center of the common reference frame. The orientation that minimizes the error between the points is then computed by the closed form solution proposed by [24].

V. SCAN REDUCTION

Modern laser scanners are virtually unlimited with respect to resolution. They can acquire more than a million points per second. A simple scan often takes a few minutes to finished. Therefore, a large number of points are available in each scan. Scan reduction becomes necessary to efficiently process the data, e.g. registration.

A. POINT BASED SCAN REDUCTION

Given a large number of points from a laser scan we propose to uniformly subsample the entire point cloud to reduce the number of points. This is achieved by first binning the point cloud in a regular 3D grid and then randomly selecting a number of points in each voxel. Both the number of points and the side length of a voxel can vary to allow for many different point densities. An additional advantage of the uniformity of the subsampling is that surfaces closer to the scanner do not unfairly influence the quality measure more than surfaces that are farther away. In [25] we describe a spatial data structure called octree with a low memory consumption. An octree is a tree data structure for indexing 3D data. Each node of the octree represents a rectangular cuboid volume. Each node can have up to eight children. Each child corresponds to one octant of the cube. A node without a child implies that no further subdivision is necessary for the corresponding volume and it can be uniformly represented. Storing a point cloud in an octree has a stopping rule for the accepted volume. The stopping criteria is defined as both maximal depth and minimal number of points. All nodes without children are considered as empty space. Since laser scanners sample the surface of objects, the 3D point cloud is not fully volumetric. Therefore, most octree nodes will only have few children. The octree data structure is ideally suited for 3D point clouds. To reduce the data we select a fixed number of points from each voxel. This will remove more points in voxels close to the scanner than in the voxels further from the scanner. After reduction the points will be uniformly distributed across the scanned environment. This is ideal for point based registration. Point based scan reduction is not suitable for panorama based registration. When creating a panorama image equally sized areas will be mapped onto differently sized areas in the panorama image depending on the projection type. The result of point based reduction is an even distribution in 3D space. This will lead to an uneven distribution of points in the 2D projection, with too few points in areas near to the scanner. The result is a panorama image that contains many holes.

B. PANORAMA BASED SCAN REDUCTION

For a panorama based registration we require a reduction method that reduces points based on the 2D projection. Panorama generation implicitly reduces points by discretizing the projection into a 2D grid. The 2D grid is necessarily of lower resolution than the original point cloud. This is due to the distortions inherent to the projection onto a 2D plane. Some areas will be "compressed" and others "stretched". In the latter case, the original resolution of the 3D scan is often insufficient for complete coverage of the 2D grid. Consequently, for an image without holes the overall resolution of the 2D image has to be reduced. To generate a rectilinear panorama image of a medium sized scan with 22.5 million points the resolution of the image should not exceed 3600×1000. This equates to 3.6 million points, i. e., a reduction by a factor of five. This is a more than sufficient resolution for registration. Further reduction leads to an even larger decrease of memory usage. Figure 3 shows an example of scan reduction. It is obvious that the point cloud reduced based on the octree is more evenly distributed while the panorama based reduction is a closer representation of the original data.

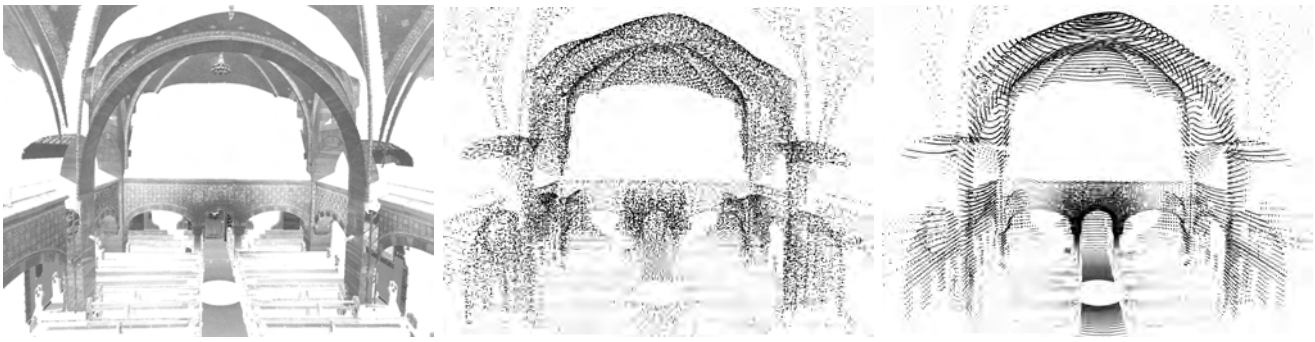

Fig. 3: Point cloud reduction. Left: original data, middle: octree based reduction, right: panorama based reduction.

We proposed three methods for panorama based scan reduction using the correspondences between panorama image pixels and 3D points in the point cloud. For the first method we project all 3D points onto the pixels of the panorama image. For each pixel we discard all points except the one with the furthest distance from the scanner thus reducing the data to at most one point per pixel. This subsampling method uses direct mapping between pixels and original point data. In the second method inverse equations are used to recover the point data from the panorama images. The original point information is lost and replaced by an approximation based on the center of the pixel and the range information of the furthest point. The reflectance information of the original point data is retained. The third method is used on top of the first two methods. After creating the panorama image conventional image resizing algorithms are applied. Due to the resizing of the image reflectance values have to be reassigned to the points as well. The different approaches used here will be explained in the experimental section.

VI. EXPERIMENTS AND RESULTS

For our experiments we implemented the three aforementioned panorama based scan reduction methods. The reduction methods were tested on data that was acquired at the campus of the Wuhan University in China with a Riegl VZ-400 laser scanner. Each scan contains around 15 million points. We compare the reduction methods with regards to their performance in panorama based scan registration. The time needed for registration is recorded as well as the success of the registration. This was decided upon visual inspection of the resulting transformation. We use the equirectangular projection in the experiments because it gives us the widest range of possible resolutions.

First we compare the first two reduction methods. The results for different resolutions of the panorama image are given in Table I. Both methods fail on images with a resolution lower than 1800×500. In these failure cases the runtime is very low. The subsampling method, i.e., selecting the furthest point per pixel from the original data, performs more reliably but also slower. The experiments show that the modification of the point coordinates using the inverse projection equations has a negative influence on the registration quality, especially with decreasing number of features.

TABLE I: Performance of reduction methods. Time is given in seconds.

Resolution	No. Points in 1,000	Subsampling			Point Recovery		
		Matches	Time	Reg.	Matches	Time	Reg.
8640×2400	10,898	235	49.67	yes	236	38.39	yes
7200×2000	8,002	392	34.69	yes	380	19.81	yes
3600×1000	2,033	141	55.43	yes	139	3.17	yes
1800×500	514	35	4.19	yes	37	0.62	no
900×250	130	16	0.48	no	15	0.14	no
450×125	32	6	0.07	no	5	0.04	no

The results of the third method on top of the others is shown in Table II. Panorama images with a resolution of 7200×2000 are scaled by the factor indicated in the first column. This is done using the scaling algorithms that are implemented in OpenCV [26]. We use both the bilinear interpolation as well as the nearest neighbor interpolation. The former is a true interpolation in the sense that new pixel values are computed, whereas the latter chooses one of the surrounding pixels in the original image as a representative. The bilinear interpolation is slower and less reliable than the nearest neighbor approach. However, the original subsampling method outperforms both of them as it registers point clouds with as little as 500,000 points while the scaling methods fail for higher point cloud sizes.

VII. CONCLUSIONS

We have shown that some of the reduction methods are very effective at drastically reducing point clouds while retaining all necessary information for panorama based registration. Reduced input sizes strongly decrease the runtime of the registration algorithm. In the future we plan to improve the results of the reduction method by applying the resizing method to the original point cloud rather than to already reduced data.

REFERENCES

[1] J. Böhm and S. Becker, "Automatic marker-free registration of terrestrial laser scans using reflectance features," in *Proceedings of 8th Conference on Optical 3D Measurement Techniques*, Zurich, Switzerland, July 2007, pp. 338–344.

TABLE II: Performance of the scaling reduction methods. Time is given in seconds.

Scale	Nearest-Neighbor Interpolation							Bilinear Interpolation						
	# points	Subsampling			Recovery			# points	Subsampling			Recovery		
	in 1,000	Matches	Time	Reg.	Matches	Time	Reg.	in 1,000	Matches	Time	Reg.	Matches	Time	Reg.
100%	8,002	392	34.69	yes	380	19.81	yes	8,002	392	34.69	yes	380	19.81	yes
75%	4,502	225	14.32	yes	205	6.73	yes	4,576	299	231.14	no	302	13.86	yes
50%	2,000	128	4.56	yes	141	3.31	yes	2,033	232	80.98	yes	234	2.88	yes
40%	1,280	95	3.11	yes	104	1.60	yes	1,301	129	34.16	no	129	1.62	yes
30%	719	52	1.21	no	58	0.86	no	732	72	12.32	no	77	1.12	no
25%	500	48	0.86	no	43	0.59	no	508	56	3.84	no	52	0.59	no

[2] H. Houshiar, J. Elseberg, D. Borrmann, and A. Nüchter, "A study of projections for key point based registration of panoramic terrestrial 3d laser scans," *Geo-spatial Information Science (GSIS)*, 2013.

[3] P. Besl and N. McKay, "A Method for Registration of 3–D Shapes," *IEEE Transactions on Pattern Analysis and Machine Intelligence (PAMI)*, vol. 14, no. 2, pp. 239 – 256, February 1992.

[4] P. Hansen, P. Corke, W. W. Boles, and K. Daniilidis, "Scale-invariant features on the sphere." in *ICCV*, 2007.

[5] P. Hansen, P. Croke, W. Boles, and K. Daniilidis, "Scale invariant feature matching with wide angle images," in *In IEEE/RSJ International Conference on Intelligent Robots and Systems*, October 2007.

[6] X. Wang, C. Toth, D. Grejner-Brzezinska, and H. Sun, "Integration of terrestrial laser scanner for ground navigation in gps-challenged environments," in *Proceedings of the XXIst ISPRS Congress: Commission V, WG 3*, 2008, pp. 513–518.

[7] M. Weinmann, M. Weinmann, S. Hinz, and B. Jutzi, "Fast and automatic image-based registration of tls data," *ISPRS Journal of Photogrammetry and Remote Sensing*, vol. 66, no. 6, Supplement, pp. 62–70, October 2011.

[8] M. Weinmann and B. Jutzi, "Fully automatic image-based registration of unorganized tls data," in *ISPRS Workshop Laser scanning 2011, ISPRS*, 2011.

[9] D. G. Lowe, "Distinctive Image Features from Scale-Invariant Keypoints," *Int. J. Comput. Vision*, vol. 60, no. 2, pp. 91–110, November 2004.

[10] H. Bay, A. Ess, T. Tuytelaars, and L. Van Gool, "Speeded-Up Robust Features (SURF)," *Computer Vision and Image Understanding*, vol. 110, no. 3, pp. 346–359, June 2008.

[11] E. Rosten and T. Drummond, "Fusing points and lines for high performance tracking." in *IEEE International Conference on Computer Vision*, vol. 2. Springer, October 2005, pp. 1508–1511.

[12] ——, "Machine learning for high-speed corner detection," in *European Conference on Computer Vision*, vol. 1, May 2006, pp. 430–443.

[13] E. Rublee, V. Rabaud, K. Konolige, and G. Bradski, "ORB: An Efficient Alternative to SIFT or SURF," *Computer Vision, IEEE International Conference on*, pp. 2564–2571, November 2011.

[14] M. Agrawal, K. Konolige, and M. R. Blas, "CenSurE: Center Surround Extremas for Realtime Feature Detection and Matching," in *ECCV (4)*, ser. Lecture Notes in Computer Science, D. A. Forsyth, P. H. S. Torr, and A. Zisserman, Eds., vol. 5305. Springer, 2008, pp. 102–115.

[15] C. Brenner, "Dreidimensionale Gebäuderekonstruktion aus digitalen Oberflächenmodellen und Grundrissen," Ph.D. dissertation, Universität Stuttgart, Fakultät fr Bauingenieur– und Vermessungswesen, 2000.

[16] K. Pathak, A. Birk, N. Vaskevicius, and J. Poppinga, "Fast Registration Based on Noisy Planes with Unknown Correspondences for 3D Mapping," *IEEE Transactions on Robotics*, vol. 26, no. 3, pp. 424–441, 2010.

[17] A. Mandow, J. L. Martinez, A. J. Reina, and J. Morales, "Fast range-independent spherical subsampling of 3d laser scanner points and data reduction performance evaluation for scene registration," *Pattern Recognition Letters*, vol. 31, no. 11, pp. 1239–1250, 2010.

[18] D. Meagher, "Geometric Modeling using Octree Encoding," *Computer Graphics and Image Processing*, vol. 19, no. 2, pp. 129–147, 1982.

[19] K. Lee, H. Woo, and T. Suk, "Data reduction methods for reverse engineering," *The International Journal of Advanced Manufacturing Technology*, vol. 17, no. 10, pp. 735–743, 2001.

[20] D. Suter and E. Lim, "Conditional Random Field for 3D point clouds with Adaptive Data Reduction," *Cyberworlds*, 2007.

[21] A. Swadzba, A.-L. Vollmer, M. Hanheide, and S. Wachsmuth, "Reducing Noise and Redundancy in registered Range Data for Planar Surface Extraction," in *ICPR*. IEEE, 2008, pp. 1–4.

[22] T. K. Sharpless, B. Postle, and D. M. German, "Pannini: A New Projection for Rendering Wide Angle Perspective Images," in *Computational Aesthetics in Graphics, Visualization, and Imaging*, 2010, pp. 9–16.

[23] M. A. Fischler and R. C. Bolles, "Random sample consensus: a paradigm for model fitting with applications to image analysis and automated cartography," *Communications of the ACM*, vol. 24, no. 6, pp. 381–395, June 1981.

[24] B. K. P. Horn, "Closed-form solution of absolute orientation using unit quaternions," *Journal of the Optical Society of America A*, vol. 4, no. 4, pp. 629–642, April 1987.

[25] J. Elseberg, D. Borrmann, and A. Nüchter, "One Billion Points in the Cloud – An Octree for Efficient Processing of 3D Laser Scans," *ISPRS Journal of Photogrammetry and Remote Sensing (JPRS)*, vol. 76, pp. 76–88, February 2013.

[26] G. Bradski and A. Kaehler, *Learning OpenCV, Computer Visoin with OpenCV library*, 1st ed. O' Reilly Media, 2008.